90th Commemorative Account: Fascinating Molecules and Reactions
Award Account
The Chemical Society of Japan Award for Creative Work for 2015

Trioxotriangulene: Air- and Thermally Stable Organic Carbon-Centered Neutral π-Radical without Steric Protection

Yasushi Morita,*[1] Tsuyoshi Murata,[1] Akira Ueda,[2] Chiaki Yamada,[3] Yuki Kanzaki,[4] Daisuke Shiomi,[4] Kazunobu Sato,[4] and Takeji Takui[4]

[1]Department of Applied Chemistry, Faculty of Engineering, Aichi Institute of Technology, Toyota, Aichi 470-0392, Japan

[2]The Institute for Solid State Physics, The University of Tokyo, Kashiwa, Chiba 277-8581, Japan

[3]Department of Chemistry, Graduate School of Science, Osaka University, Toyonaka, Osaka 560-0043, Japan

[4]Department of Chemistry and Molecular Materials Science, Graduate School of Science, Osaka City University, Sumiyoshi-ku, Osaka 558-8585, Japan

E-mail: moritay@aitech.ac.jp

Received: March 5, 2018; Accepted: March 15, 2018; Web Released: May 28, 2018

Yasushi Morita
Yasushi Morita received his Ph.D. in 1989 from Nagoya University under the supervision of Prof. Ryoji Noyori. After spending one year as a Postdoctoral Fellow at Prof. Stuart Schreiber's Lab at Harvard University, he joined Prof. Nakasuji's Lab as a Research Associate at Institute for Molecular Science. In 1993 he moved to Osaka University as Assistant Professor, and then he was promoted to Lecturer in 2003 and Associate Professor at Osaka University in 2004. He was then appointed as a professor at Aichi Institute of Technology in 2014. His research interests focus on the exploration of delocalized π-electronic systems based on synthetic and physical organic chemistry, especially air-stable neutral radicals, hydrogen-bonded charge-transfer complexes, and supramolecular self-assemblies as well as applications for organic batteries and quantum information technology including dynamic nuclear polarization.

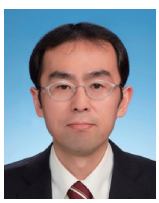

Tsuyoshi Murata
Tsuyoshi Murata graduated from Osaka University in 2000 and received his M.Sc. in 2002 and Ph.D. in 2005 under the guidance of Prof. Kazuhiro Nakasuji. After receiving his Ph.D. degree, he worked as a postdoctoral fellow at Kyoto University with Prof. Gunzi Saito and Prof. Hideki Yamochi in 2005–2009, and at Osaka University with Prof. Yasushi Morita in 2009–2013. In 2013–2015, he worked at ChemGenesis Inc. and Tokyo Chemical Industry Co., Ltd. In 2015, he moved to Aichi Institute of Technology as an associate professor. His research interests focus on the exploration of molecular assemblies with exotic properties and functions based on physical organic chemistry, especially organic conductors, proton-electron cooperative systems, and stable neutral π-radicals.

Akira Ueda
Akira Ueda was born in 1982 in Ishikawa, Japan. He received his B.Sc. degree (2005) from Osaka University under the supervision of Prof. Kazuhiro Nakasuji and Prof. Yasushi Morita, and then obtained his M.Sc. (2007) and Ph.D. (2010) degrees from the same university under the supervision of Prof. Yasushi Morita. He then became a postdoctoral fellow in Prof. Morita's group, and since January 2012, he has been a research associate at the Institute for Solid State Physics (ISSP), The University of Tokyo (Prof. Hatsumi Mori's group). His current research interests focus on the development of novel functional molecular materials, such as organic conductors, semiconductors, and magnetic and dielectric materials, based on the design and synthesis of new organic molecules. He has received the ISSP Young Scientist Medal (2016) and the CSJ Award for Young Chemists (2016).

Yuki Kanzaki
Yuki Kanzaki received his doctoral degree from Osaka City University in 2006 under the supervision of Prof. Takeji Takui. Then he was a postdoctoral researcher at Osaka City University (2006–2008, 2010–2015) and Osaka University (2009–2010). Currently, he is working at the Osaka City University as a specially appointed lecturer. His present research focuses on physical properties of organic molecule-based magnets and rechargeable batteries.

Daisuke Shiomi
Daisuke Shiomi was born in Kyoto, Japan in 1965. He received his B.Sc. in 1988 and D.Sc. in 1993 from the Univ. Tokyo. He joined Prof. Koichi Itoh's group at Osaka City Univ. as a research associate. He has been working as an associate professor in collaboration with Prof. Takeji Takui and Prof. Kazunobu Sato at Osaka City Univ. His current research interest is focused on magnetic properties of molecule-based materials.

Kazunobu Sato
Kazunobu Sato received his Doctor of Science from Osaka City University in 1994 under the supervision of the late Prof. Koichi Itoh. Then he joined Prof. Takui's laboratory at Osaka City University as Assistant Professor, where he studied organic high-spin molecules as models for purely organic magnets in terms of single-crystal ESR/ENDOR spectroscopy and pulse-ESR based two-dimensional electron spin transient nutation (2D-ESTN) spectroscopy. He was promoted to Associate Professor in 2002, and to Professor in 2006 at Graduate School of Science, Osaka City University. His current research interests are molecular spin quantum computers and related quantum spin technology based on pulse-based ESR. He has been applying advanced ESR spectroscopy to molecular synthetic chemistry to manipulate the microscopic quantum nature of molecular open-shell systems.

Takeji Takui
Takeji Takui received his Dr. Eng., from Osaka Univ. under the supervision of the late Profs. Koichi Itoh and Noboru Mataga, Chem. Div./Dept. of Chem., School of Eng. Sci., Osaka University in 1973, joining Prof. C. A. McDowell's group, UBC., Vancouver as PD (teaching & research) for 1974–78 after working at Osaka Univ. as JSPS PD until 1974. He was appointed as Assistant Prof. at Chem. Dept., Fac./Graduate School of Sci., Osaka City University (OCU) in 1978, being promoted to Lecturer in 1986, Associate Prof. in 1989 and Professor in 1992. He was allowed to hold the title of Emeritus Prof., OCU in 2007, and kept working as Specially Appointed Prof./Senior URA at OCU until now. His main interests emphasize open shell chemistry such as molecular design and characterization of topological high spin π-electron network systems, as underlain by advanced electron magnetic resonance/its generalized methodology, and quantum chemistry for molecular magnetic properties (ZFS and g-tensors) relevant to spin-orbit interactions. For the last twenty years his interests focus on the implementation of molecular-spin based quantum computers/quantum information processing, practical quantum algorithms for quantum chemistry and molecular-spin mediated direct energy conversion devices.

Abstract

To stabilize organic neutral radicals, which are usually very unstable chemical species in air atmosphere, "steric protection" is the most general and indispensable method. Based on the design of electronic-spin structure of polycyclic carbon-centered π-radicals, we have for the first time realized a peculiarly stable neutral π-radical without bulky substituent groups, 4,8,12-trioxotriangulene (**TOT**), whose decomposition point is higher than 240 °C in the solid state under air. This remarkably high air-stability as a neutral radical is achieved by spin-delocalization originating from the symmetric and expanded π-electronic structure of **TOT**. The oxo-functionalities also highly contribute to the high stability through electronic-spin modulation, where the largest electronic spin density located at the central carbon atom further decreases the spin densities of the peripheral carbon atoms. In the solution state, **TOT** is in the equilibrium between the monomer and highly symmetric π-dimer, as stabilized by the formation of the strong two-electron-multicenter bonding. Crystal structure analysis revealed that **TOT** derivatives show strong self-assembling ability forming one-dimensional columns, which further construct three-dimensional networks by multiple intercolumnar non-covalent interactions due to the absence of bulky substituent groups. Substituent groups at the apexes of the triangular carbon-framework of **TOT** afford variations of the π-stacking mode in the one-dimensional columns, influencing the magnetic properties and photo-absorptions around the near-infrared region. The electronic effect of the substituent groups also affects the redox potentials of **TOT**. The peculiarly high stability of **TOT** neutral radicals and their three-dimensional

networks by robust intermolecular interactions achieved in our study are very beneficial for the molecular design of new polycyclic air-stable neutral radicals. Furthermore, we believe that the open-shell electronic structures of neutral π-radicals, which are quite different from those of close-shell molecular systems, will also produce milestones for the exploration of peculiar physical properties and catalytic activity for organic transformation originating from their unconventional electronic-spin nature.

Keywords: Stable organic radical | Fused π-electronic system | Electronic spin structure

1. Introduction

Organic neutral radicals are known as intermediates and catalysts of various chemical reactions, and are highly reactive and unstable species due to the unpaired electron.[1] Besides such chemical viewpoints, the electronic-spin and redox activity of radicals inherent in their open-shell electronic structure have attracted much attention as potential sources of electronic materials.[2] The most essential and serious barrier for the synthesis and application of organic neutral radicals is the instability causing mainly σ-dimerization and reaction with O_2. The most popular and effective method to obtain stable neutral radicals is kinetic stabilization by surrounding the radical center with bulky groups (steric protection).[2] However, this method also suppresses intermolecular interactions essential for solid-state electronic functions such as electronic transport and strong intermolecular magnetic interactions. Furthermore, the steric protection restricts the variation of chemical modifications indispensable for the expansionary functionalities such as electronic spin structure, redox properties, and molecular arrangement in the solid state.

In the case of π-radicals, where the radical center is included in a π-conjugated system, the delocalization of electronic spin increases the thermodynamic stability. Phenalenyl (**PNL**), an odd alternant hydrocarbon-based neutral π-radical with D_{3h} symmetry having a 13π electronic system, possesses a highly delocalized electronic-spin structure (Figure 1).[3,4] The α-carbon atoms possess larger spin densities generating reactive sites, and **PNL** radical is in equilibrium with a σ-dimer in solution.[5] Therefore, the steric protection with bulky substitutent groups such as *tert*-butyl, halogen, and methoxy groups is required for the isolation of **PNL** radicals.[6,7] Stabilization of **PNL** radical has also been achieved by introducing the zwitterionic functionality seen in bis**PNL** boron complexes[8] and further π-extension in a **PNL** dimer system.[9] Besides these carbon-centered π-radicals, heteroatom-centered π-radicals such as thiazyl-type[2a] and Blatter-type[10] neutral radicals also show high stability due to the spin delocalization effect of heteroatoms. Focusing on the delocalized electronic spin nature, we have investigated various **PNL**-based neutral π-radicals with heteroatomic substitution[4,11,12] and π-extension.[13a] Such chemical modifications in carbon-centered π-radicals drastically varied the electronic-spin structures, and highly affected the stability, molecular structure of decomposition products, and physical properties.

4,8,12-Trioxotriangulene (**TOT**, **1**), a neutral π-radical possessing a 25π electronic system, can be designed by the 2D π-

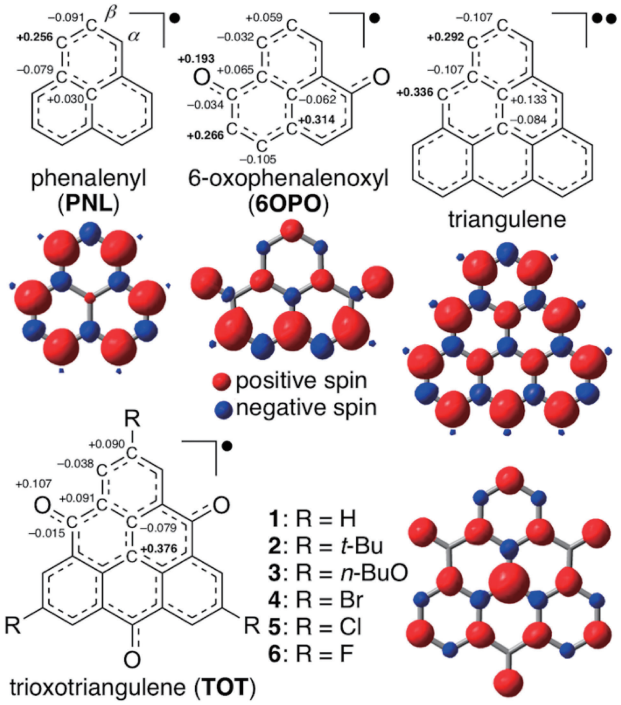

Figure 1. Molecular and electronic-spin structures of triangular polycyclic carbon-centered π-radicals. Electronic-spin densities were obtained by DFT calculation at a UBLYP/6-31G** level. Numerical values with the molecular structures are the electronic spin densities on each C and O atom. The values of symmetrically equivalent atoms are averaged. Bold numbers represent the atoms possessing relatively large spin densities.

extension and three-oxo functionalization of **PNL**, and is also regarded as a hybrid system of triangulene and **6OPO**.[14,15] Interestingly, Alison and coworkers synthesized the monoanion species of **1**, and succeeded in the generation of its radical dianion and diradical trianion species,[16] however, the neutral radical **1** was not synthesized.[17] The DFT calculation of **TOT** indicates that the electronic spin delocalizes over the whole π-electronic system, and the largest density locates at the central carbon atom, which suggests high stability. Figures 1 and 2 show the spin distribution of **TOT** neutral radical calculated by us, that coincides with the result of Ikabata's work.[17] Atomic spin densities at the central and peripheral carbon atoms are 0.38 and 0.04–0.09, respectively (Figure 1), the latter of which are much smaller than those of the reactive sites of **PNL** (0.26), triangulene (0.34), and **6OPO** (0.27). The spin distribution nature suggests that the peripheral carbon atoms of **TOT** are less reactive. Since the σ-bond formation at the central carbon atom of **TOT** may induce a severe distortion of the π-conjugated electronic system, the atom is hardly expected to undergo σ-dimerization and oxidation. We have previously synthesized **TOT** derivatives having *tert*-butyl, *n*-butoxy and bromo groups at the 2,6,10-positions (**2**–**4**, respectively, sites having the largest spin densities among the peripheral carbon atoms) as stable neutral radical species.[14,15] These derivatives were treatable under air at room temperature, and did not show any decomposition at least to 250 °C in air. In addition to such a remarkable high stability, the multi-stage redox ability

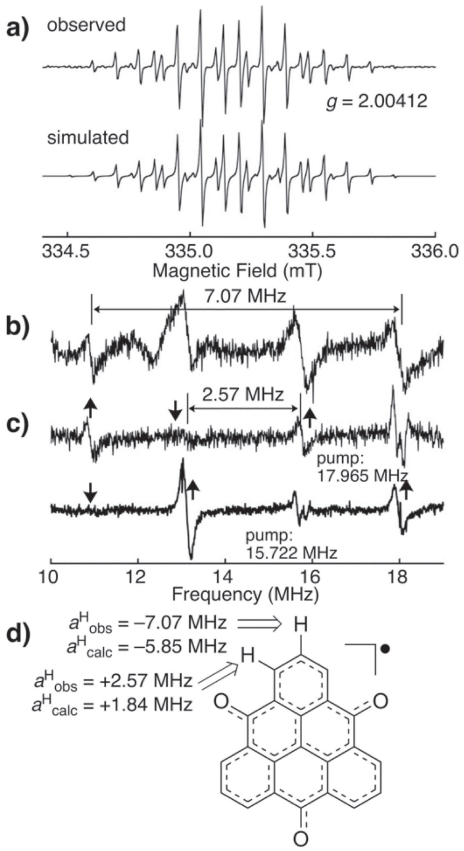

Figure 2. ESR spectra of **1** in toluene (1×10^{-4} M). (a) Observed and simulated hyperfine EPR spectra at 293 K. The microwave frequency used: 9.4015607 GHz. (b) ^{1}H-ENDOR and (c) ^{1}H-TRIPLE spectra at 273 K. In (c), up and down arrows denote the increase and decrease in ENDOR intensity at the resonance frequency during pumping at the transition due to the hydrogen atom. (d) Observed (top) and calculated (bottom) hfcc values (a^{H}). Calculation was carried out at the UBLYP/6-31G** level of theory.

of **2** and **4** originating from the extremely narrow energy gap between singly occupied molecular orbital (SOMO) and doubly degenerate lowest unoccupied MO (LUMO) realized high performance as electrode active materials of Li-ion secondary batteries.[14] Furthermore, neutral radicals, where two or three oxygen atoms of **2** were substituted with dicyanomethylene groups, also showed similar spin density distributions and high stabilities.[18] To investigate the excellent stability of **TOT** system and the substituent effects on the physical properties, we have prepared and characterized the non-substituted **TOT** neutral radical **1** and its 2,6,10-trichloro and trifluoro derivatives (**5** and **6**, respectively) having smaller substituent groups than bromo- and *n*-butoxy groups, aiming towards expansionary materials functionalities.

2. Results and Discussion

Synthesis and Stability. The tetrabutylammonium salt of the anion species of **TOT** derivatives **1**,[16b] **5** and **6** were synthesized by the same method as **4** in our previous paper,[14a] and the detailed procedure is described in Supporting Information. Neutral radicals **1**, **5**, and **6** were prepared by oxidation of the anion salts using 2,3-dichloro-5,6-dicyanobenzoquinone (DDQ). The electrochemical oxidation of the anion salts in appropriate solvents also gave a crystalline sample of neutral radicals suitable for the structural analyses (Figure S1). The *n*-butoxy and fluorinated derivatives **3** and **6**, respectively, were soluble in various organic solvents such as halogenated solvents (CH_2Cl_2, $CHCl_3$, 1,1,2,2-tetrachloroethane) and toluene, and the solubility of *tert*-butyl derivative **2** in these solvents was lower than **3** and **6**. The solubility of non-substituted **1** was further poor, and only slightly soluble in toluene, and the solution state UV-vis measurement was performed for the filtrate of the reaction mixture of oxidation of the monoanion salt using PbO_2 (see caption of Figure S4). The brominated **4** and chlorinated **5** were insoluble in any organic solvent, due to the robust intermolecular halogen-bonds as seen in the crystal structures (*vide infra*).

All the neutral radicals **1**–**6** were stable in the solid state under air at room temperature, and the decomposition points, which were determined by the blackening of powdered samples with heating under air, were higher than 240 °C. In the thermogravimetric analysis of **1**–**6** under N_2 atmosphere, distinctive decrease of the sample weight was not observed until 350 °C, indicating high thermal stability (Figure S2). It should be noted that the powdered sample of **1** heated at 350 °C under air, at which the brown color of **1** became black, showed an IR spectrum exactly the same as the original sample (Figure S3). Such an observation indicates that only the surface of the powder decomposed due to air-oxidation, and most of the sample survived the high temperature.

Surprisingly, the pristine **TOT 1** showed an efficiently high stability for handling even in solution. In the degassed solution, **TOT** neutral radicals did not show a decrease of the ESR signal intensities, suggesting decomposition due to σ-dimerization, for several days. On the other hand, **1** in solution under air slowly decomposed as observed in the temporal observation of UV-vis spectra (Figure S4). From the decay of absorption bands, the half-life of **1** in a saturated 1,1,2,2-tetrachloroethane solution under air at room temperature was determined to be 18.5 days, which is longer than that of the π-extended **PNL** dimer (2.5 days) determined by a similar method.[9a] The introduction of bulky substituent groups R at the 2, 6 and 10 positions enhances stability, and **2** having three bulky *tert*-butyl groups further possessed a longer half-life of 56 days (Figure S5). The distinguishable stability of *n*-BuO derivative **3** also indicates the importance of the electronic effect of substituent groups on the stability of **TOT** neutral radicals (Figure S6). Delocalization of electronic spin on the substituent groups reduces the electronic-spin density on the **TOT** skeleton, and would result in the further stabilization of **3**. The calculated electronic-spin density on the substituent groups of **3** was largest among **1**–**6** (Table S1).

Electronic-Spin Structure and π-Dimerization in the Solution State. Figure 2a shows the observed and simulated ESR spectra of **1** in toluene, showing a well-resolved multiline spectrum originating from the hyperfine couplings with the six and three hydrogen atoms at the α- and β-positions, respectively. The hyperfine coupling constants (a^{H}) of the α- and β-hydrogen atoms determined by ^{1}H ENDOR/TRIPLE spectros-

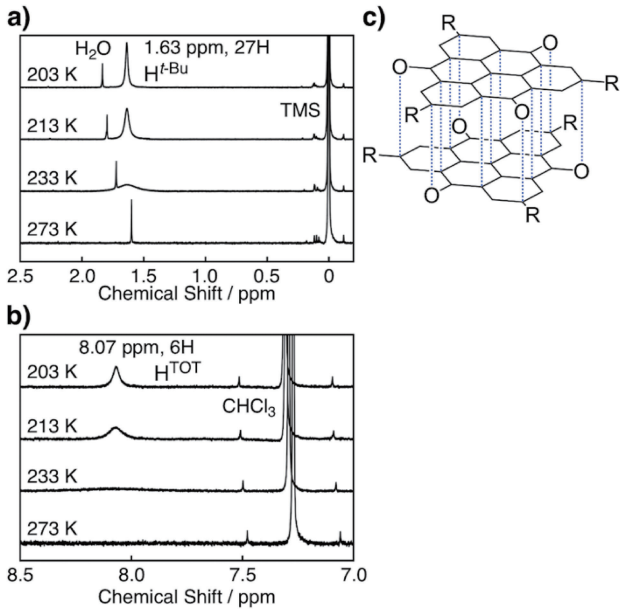

Figure 3. (a,b) Temperature-dependent ^{1}H NMR spectra of **2** in a $CDCl_3$ solution (1×10^{-3} M) in the aliphatic (0–2.5 ppm) and aromatic (7.0–8.5 ppm) regions, respectively. (c) Schematic drawing of 2-electron-26-center bonding in the π-dimer of **TOT**.

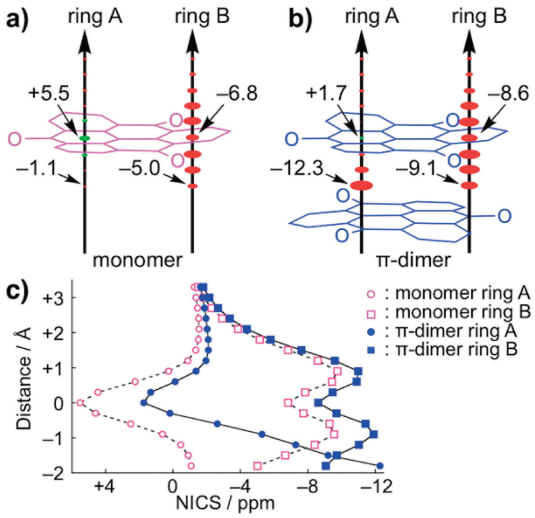

Figure 4. Out-of-plane NICS distributions at the centers of ring-A and -B in (a) monomer and (b) π-dimer of **2** at an interval of 0.6 Å. The radius of each red circle corresponds to the magnitude of each negative NICS. (c) A plot of the NICS values as the function of out-of-plane distance with an interval is 0.3 Å. The calculation was performed at the UB3LYP/6-31G(d) level of theory using the molecular geometries in the crystal structure at 93 K.[20]

copy (Figures 2b and 2c) were +2.57 and −7.07 MHz, respectively. These values were successfully assigned with the help of DFT calculations, suggesting that the unpaired electron of **1** delocalizes over the whole π-electronic system with three-fold symmetry as seen in the calculated spin density distribution (Figures 1 and 2d). The a^H value of the α-hydrogen atoms in **6** experimentally determined by the ESR measurements was +2.55 MHz (Figure S9), and very similar to those of **1** and **2**.[15] The DFT calculation of **6** suggested that the electronic spin delocalizes to the fluorine atoms, however, the electronic spin densities on the carbon and oxygen atoms of the **TOT** skeleton were very similar to those of **1** and **2** (Table S1). These results indicate that the effect of halogen atoms at the β-positions on the electronic spin structure of **TOT** skeleton is small. The intensity of the ESR signal of **1** gradually decreased upon cooling due to the π-dimerization as observed in **PNL** radicals (Figure S8).[19] Such ESR features were also observed for **2**[17] and **6** (Figure S10), indicating the strong multicenter bonding nature in the **TOT** π-dimer with a staggered pattern (Figure 3a).[19]

The highly symmetric π-dimeric structure of **2** in the solution state was proved by temperature-dependent ^{1}H NMR spectroscopy in a $CDCl_3$ solution (1×10^{-3} M). At 273 K, no NMR signals derived from **2** species were observed due to the paramagnetic effect of the unpaired electron. At low temperature, the concentration of the non-magnetic π-dimer increased, and two broad signals appeared around 1.63 and 8.07 ppm (Figures 3a and 3b, respectively). These signals became sharp with lowering temperature, and the ratio of the signal intensities at 1.63 and 8.07 ppm was 27:6, suggesting that they are attributable to the hydrogen atoms of three *tert*-butyl groups and six aromatic C–H groups, respectively. This appearance/disappearance of the signals was observed reversibly upon cooling and heating. The observed behavior of **2** in the NMR spectrum well coincides with that observed in *tert*-butyl **PNL** radical,[19b] and indicates that **2** forms a diamagnetic π-dimer having a three-fold symmetry in the solution state (Figure 3c). The signals calculated by the DFT method were 1.69 and 8.28 ppm for the hydrogen atoms of three *tert*-butyl groups and six aromatic C–H groups, respectively, and close to the observed values.

To evaluate the effect of π-dimerization on the aromaticity of **2**, the nucleus-independent chemical shift (NICS) was calculated.[20] The NICS values of the centers of rings-A and -B in monomeric **2** were +5.5 and −6.8 ppm, indicating that ring-B exhibits higher aromaticity (Figure 4a). Both of these values showed a significant negative shift in the π-dimer of **2**, +1.7 and −8.6 ppm for rings-A and -B, respectively (Figure 4b), suggesting the enhancement of aromaticity by the π-dimerization. A similar trend of the enhancement was more pronounced in the interior of the π-dimer (Figure 4c), suggesting the robustness and thermodynamic stability of the π-dimer of **2** with the nature of 26-center-2-electron multicenter bonding.

The π-dimerization was also found in the UV-vis spectra, where a low energy band around 700–1000 nm assignable as the intermolecular charge-transfer absorption appeared on lowering temperature (Figure S11, see also ref. 16). The appearance of this band is additional evidence of the π-dimerization of **TOT**, since the σ-dimerization cut off the π-electronic system into several pieces and would causes the appearance of shorter wavelength absorption bands.[12,15,19]

Crystal Structures. In the crystal structure of **1**, the molecule possesses a three-fold axis, and 1/3 of the molecule is crystallographically independent (Figure S12). The intramolecular C–C bond lengths excepting those of neighboring C–O bonds were 1.385–1.439 Å (Table S2) and comparable to those of **PNL** radicals[6a] and naphthalene. The C–C bonds

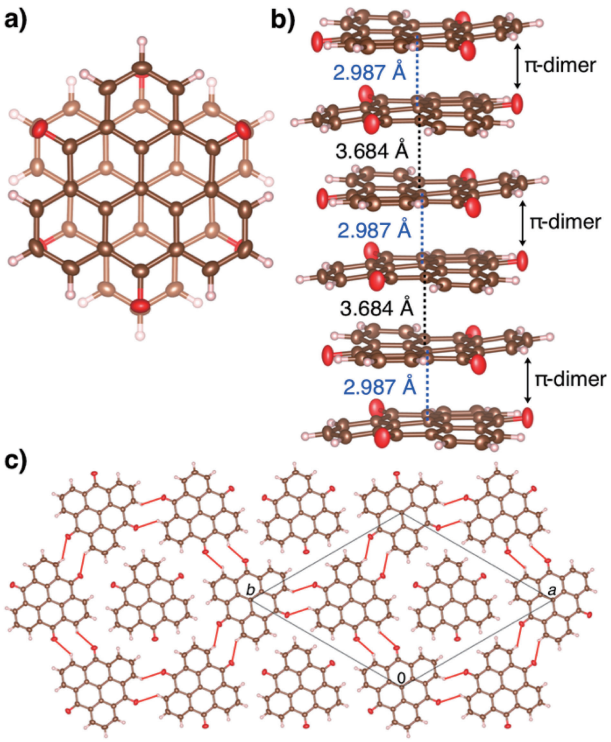

Figure 5. Crystal structure of **1**. (a) Overlap pattern in the π-dimer of **1**. (b) One-dimensional column along the c-axis by the stacking of the π-dimers. (c) Two-dimensional C–H···O interactions (red lines, 2.69 Å) in the $0 < c < 0.5$ layer viewed along the *c*-axis.

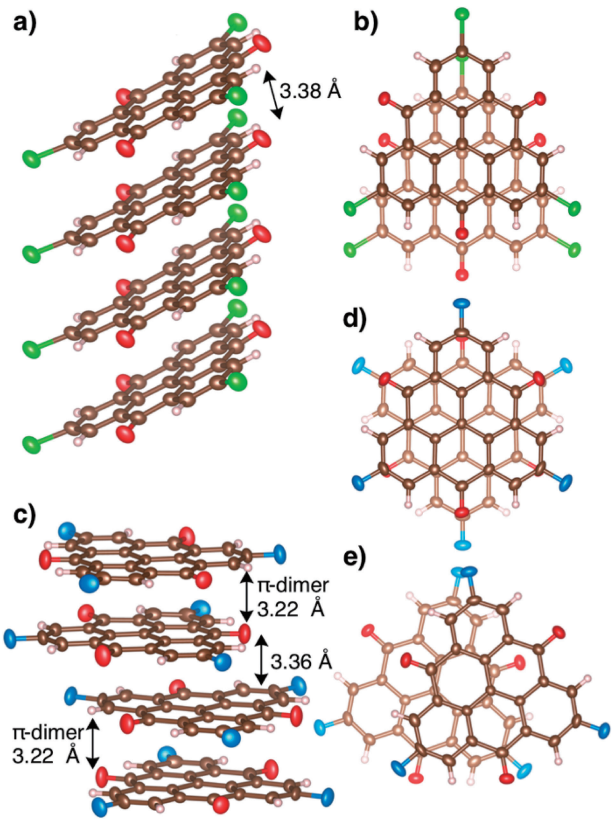

Figure 6. Crystal structures of **5** and **6**. (a) Uniform one-dimensional π-stacking column of **5**, and (b) a slipped-stack overlap pattern in the column. (c) One-dimensional π-stacking column of **6**, and overlap modes in the column, (d) interdimer and (e) intradimer stacking modes.

neighboring carbonyl groups (1.485 and 1.482 Å) were longer than the other bonds, corresponding to the small spin population at C4, C8 and C12 atoms. The bond length analysis supports the extensive delocalization of electronic spin on the **TOT** skeleton shown in Figures 1 and 2. The overall features in the intramolecular bond lengths are very similar among **TOT** derivatives **1**–**6** (Table S2) and also their anion species (Table S3). These results clearly indicate that the **TOT** neutral radicals exist as a discrete molecular species in the solid state.

The self-assembling ability of **TOT** derivatives originating from the strong intermolecular multiple SOMO–SOMO interaction within the face-to-face π-stacks constructs one-dimensional columns.[14,15] The face-to-face stacking of **1** formed a π-dimer with a staggered overlapping pattern (Figure 5a), where spin-rich carbon atoms are close to each other to strengthen the SOMO–SOMO interaction forming a 2-electron-26-center ($2e^-$/26C) bond (Figure 3c).[4] The **TOT** skeleton had a slightly bowl-like shape with a bend to shorten the distance of the central carbon atoms having the largest electronic spin population. The resulting central C–C distance, 2.987 Å, was extremely shorter than the sum of van der Waals radii of two other carbon atoms (3.40 Å).[21] The π-dimer of **1** further stacked to form a one-dimensional column along the *c*-axis (Figure 5b). The stacking pattern between the π-dimers is a staggered mode the same as the intradimer one, and the central C–C distance was 3.684 Å. These structural features are very similar to those of **2**, where the intra- and interdimer and central C–C distances are 2.979 and 3.641 Å, respectively.[14,15] Since **1** does not possess bulky substituent groups, the one-dimensional column more densely arranged in the crystal than **2** having three *tert*-butyl groups.[14] Multiple intercolumnar C–H···O type hydrogen-bonds formed a two-dimensional structure parallel to the *ab*-plane (Figure 5c). Such a three-dimensional network by the non-covalent interactions strengthens the molecular packing, and causes the decreased solubility in common organic solvents that is favorable for implementing the cycle performance of lithium ion secondary batteries using **TOT** as the cathode active material.[14]

The π-stacking structures of **TOT** derivatives were highly affected by the substituent groups R. The chlorinated **5**, which was isostructural to **4**,[14] formed a uniform column with a slipped stacking and an interplanar distance of 3.38 Å (Figures 6a and 6b). In the column of fluorinated **6**, the staggered-type π-dimer further stacked with a twisted stacking (Figures 6c–e). It should be noted that the intercolumnar interactions involving halogen atoms were formed in the crystal structures of **4**–**6**, modulating the stacking patterns within the π-stacking columns (Figures S13 and S14).

In the π-dimers of **TOT** derivatives, the unpaired electrons on each **TOT** monomer couple through the $2e^-$/26C bond to form a close-shell electronic state. The strong tendency of **TOT** neutral radicals to form π-dimers may contribute to their high air-stability in the solid state.

Solid State Properties. The effect of these structural differences can be distinctly shown in the solid-state electronic

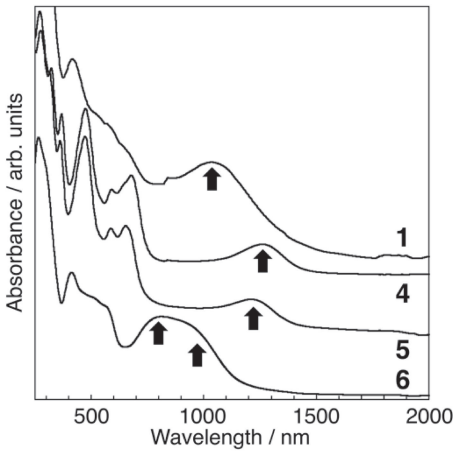

Figure 7. Solid state electronic spectra of **1** and **4**–**6** in KBr. Black arrows indicate the peak tops of the intermolecular charge-transfer bands.

spectra, which show characteristic near-infrared absorption bands assignable as the intermolecular transition within the column (Figures 7 and S15).[15] The strongly dimerized column of **2** with a staggered stack shows the band at 1134 nm. In the case of the pristine **TOT 1** forming a dimerization and stacking pattern similar to **2**, the band appeared at 1030 nm, whose blue-shift in comparison with that of **2** was caused by the delocalization of SOMO into substituent groups as suggested by theoretical calculation.[15] The column of **6** having a twisted stacking between the staggered-type π-dimers showed two bands around 800 and 1000 nm. In the cases of **4** and **5** having uniform π-stacking columns, the intermolecular absorption bands were observed at 1250–1300 nm, which are longer than those of π-dimerized columns of **1**–**3** and **6**. The absorption wavelengths of these bands were also longer than that of tris(perfluorophenyl)**PNL** radical (700–800 nm) which forms a uniform π-stacking column with a long distance of 3.65 Å.[5c] A uniform π-stacking of radicals likely to be **4** and **5** can be characterized as a one-dimensional electron-correlated system, and the photo-absorption energy can be interpreted with the difference between on-site and nearest-neighbor Coulomb repulsions, U and V, respectively, $(U - V)$.[22] The low-energy absorptions of **4** and **5** were caused by the expanded π-electronic system of **TOT** reducing U and the strong intermolecular π-π interaction increasing V.

In the temperature dependence of magnetic susceptibility (χ_p), almost all spins of **1**–**3** were quenched due to the strong antiferromagnetic interaction within the π-dimers, and the χ_pT values slightly increased with increasing temperature at high temperature regions (Figures 8a and S16a). The analysis of **1** and **2** based on the singlet-triplet model[23] resulted in the $2J/k_B > -2000$ K of antiferromagnetic interactions. In the case of **3**, where the interaction between π-dimers was larger than **1** and **2**,[15] the temperature dependence of χ_p can be explained by the alternating antiferromagnetic chain model[24] with the intra- and inter-dimer interactions of $2J/k_B = -2000$ K and -1120 K, respectively (Figure S16b). The χ_pT value of **4** at 300 K was 0.234 emu K mol^{-1} which corresponds to 62% active spins for $S = 1/2$, and monotonously decreased with temperature (Figure 8b). The temperature dependence of χ_pT was reproduced by the uniform 1D model[25] with an antiferromagnetic interaction $2J/k_B = -159$ K within the column. The peculiarly weak antiferromagnetic interaction in **4** having a slipped stacking pattern was expected in the quantum chemical calculation reported by Kinoshita *et al.*[26a] Surprisingly, no abrupt spin-quenching caused by spin-Peierls transition which is common to 1D radical arrays[27] was observed down to 2 K. Although intercolumnar overlap integrals are small, electrostatic Br···O and C–H···O interactions would increase the rigidity of the 3D crystal structure and stabilize the uniform stacking disturbing lattice deformations.

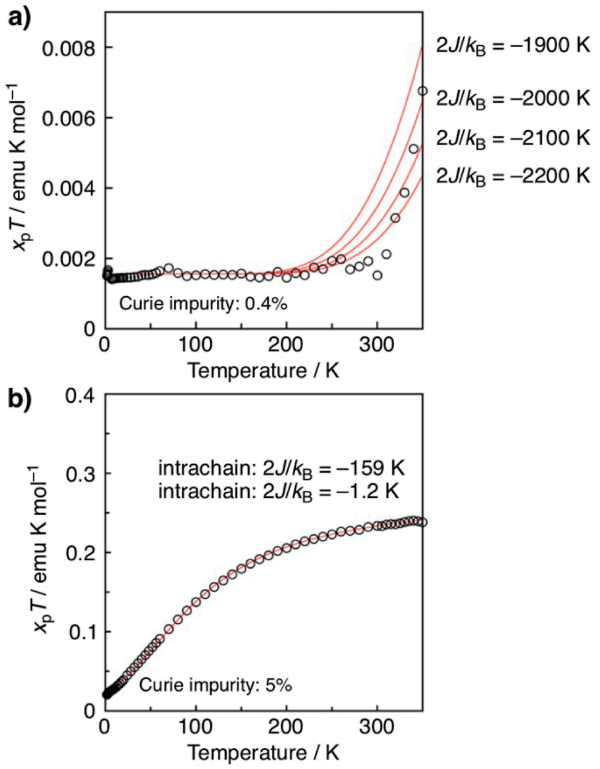

Figure 8. Temperature dependence of χ_pT of (a) **1** and (b) **4** (open circles). The red lines are the fitting results obtained by Bleaney-Bowers[23] and Bonner-Fisher[25] models, respectively.

Redox Properties. The substituent effect on the electronic properties of **TOT** was evaluated by redox behaviors from the measurement of cyclic voltammetry of the corresponding monoanion species in DMF solution. Pristine **1** exhibited four redox processes from neutral radical to radical tetraanion species (E^1 to E^4), where $E^1 = -0.05$ V (vs Fc/Fc$^+$, peak potential) and $E^4 = -3.09$ V were irreversible probably due to the low solubility, and $E^2 = -2.10$ V and $E^3 = -2.45$ V were reversible (Figure 9). The E^1 values of **2** and **3** having electron-rich substituent groups were -0.26 and -0.38 V, respectively, and significantly lower than that of **1** (Figure S17). In the case of halogenated derivatives **4**–**6**, the electron-withdrawing ability of the substituent groups caused the ~0.4 V of positive shifts in the E^2–E^4 processes (Figure S17).

3. Conclusion

In conclusion, we for the first time have realized a peculiarly stable neutral π-radical of **TOT** without bulky substituent

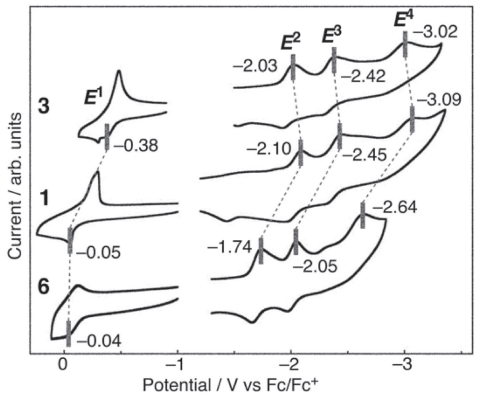

Figure 9. Cyclic voltammograms of **1**, **3** and **6** measured using their n-Bu_4N^+ salts of monoanion species (5 mM) in DMF solution. The results were calibrated with ferrocene/ferrocenium couple (Fc/Fc^+). Peak potential was listed because of the irreversibility of the E^1 and E^4 processes.

groups. It can be handled in air in both solution and solid states, and its decomposition point in the solid state is higher than 240 °C in air. Such high stability of **TOT** as a neutral radical was underlain by the high spin delocalization over the entire highly symmetric π-electronic skeleton where the largest spin density locates at the central carbon atom. The molecular design is based on the topological symmetry control in the electronic-spin distribution, and the importance of sizable spin delocalization in stabilizing extended π-radicals is demonstrated. It should be noted that the absence of steric hindrance enables **TOT** neutral radicals to interact with neighboring molecules without the σ-bond formation, resulting in the construction of multi-dimensional network with intermolecular non-covalent interactions in the solid state.

Our investigation on the newly demonstrated stabilization method for organic carbon-centered neutral π-radicals will highly contribute to the molecular design of new polycyclic air-stable neutral radicals. Furthermore, the remarkably high stability of **TOT** neutral radicals will provide a new material design strategy for organic electronic devices and molecular catalyst for organic transformation. The **TOT**-based high-performance secondary battery in our previous study[14] is the beginning of the development of neutral π-radical-based electronic materials. The magnetic interaction and intermolecular charge-transfer absorption bands around near-infrared region[15] indicate the strong multicentered SOMO-SOMO interaction within the columns, which is necessary for various electronic functionalities, such as electrical transport and photo responses.[15] Our further investigation on the **TOT** system is in progress for the development of new neutral radical-based materials such as electron transport, electrode-active materials, and molecular catalyst related with redox activity in not only the solid state but also thin-film.

4. Experimental

Materials. The tetra-*n*-butylammonium (***n*-Bu$_4$N$^+$**) salt of monoanion species of non-substituted **TOT** (**1**$^-$) was prepared according to the procedure described in the previous work,[14a] and the chlorinated and fluorinated **TOT** derivatives (**5** and **6**) were newly synthesized by the same method as brominated derivative **4**, which was reported in our previous paper.[14a] DDQ (2,3-dichloro-5,6-dicyanobenzoquinone) was purified by sublimation. Acetonitrile used for the electrochemical oxidation was purified by distillation from P_2O_5 followed by CaH_2. CH_2Cl_2 used for the electrochemical oxidation was purified by distillation from CaH_2. R_f values on TLC were acquired on E. Merck precoated (0.25 mm) silica gel 60 F_{254} plates. The plates were sprayed with a solution of 10% phosphomolybdic acid in 95% EtOH and then heated until the spots became clearly visible.

Material Characterization. Melting and decomposition points were measured with a hot-stage apparatus with a Yanako MP-J3, and were uncorrected. Melting and/or decomposition were detected by eye observation. The decomposition was observed by changing of the color, where the surface of powdered samples became dark above the decomposition points. Elemental analyses were performed at the Graduate School of Science, Osaka University. ESI-MS spectra were measured from solutions in MeOH on a Thermo Scientific LTQ Orbitrap XL. Electronic spectra were measured for KBr pellets or solutions on a Shimadzu UV/vis scanning spectrophotometer UV-3100PC. Infrared spectra were recorded on a JASCO FT/IR-660 Plus spectrometer using KBr pellets (resolution 4 cm^{-1}).

Thermal Analyses. Stability of **1**, **2** and **4**–**6** in the solid state was studied by thermogravimetric-differential thermal analysis (TG/DTA) using TG/DTA7300 (SII Nanotechnology Inc.). TG measurement of **3** was performed with Simultaneous Thermal Analyzer STA6000 from PerkinElmer. Samples (5–10 mg) were sealed in aluminum pans, and heated in flowing nitrogen at heating rate of 1–5 K/min. The background was subtracted by measurement of a blank cell.

Electrochemical Measurements. Cyclic voltammetric measurement was made with an ALS Electrochemical Analyzer model 630A. Cyclic voltammograms were recorded with 3-mm-diameter carbon plate and Pt wire counter electrodes in dry DMF containing 0.1 M n-Bu_4NClO_4 as supporting electrolyte at room temperature. The experiment employed a $Ag/AgNO_3$ reference electrode, and the final results were calibrated with a ferrocene/ferrocenium couple.

Magnetic Measurements. Magnetic resonance measurements of the radicals were performed in toluene at 290 K on Bruker ELEXSYS E500 spectrometer for X-band liquid-phase ESR spectra and on Bruker ESR/ENDOR spectrometers ESP 300/350 for ^{1}H-ENDOR, and ^{1}H-TRIPLE spectra equipped with a wide-band 500 W radiofrequency amplifier. The solution of the radical was degassed by the freeze-pump-thaw method before the measurements were recorded. The magnetic susceptibility was measured on a Quantum Design SQUID magnetometer MPMS-XL at 2–350 K. The magnetic responses were corrected with diamagnetic blank data of the sample holder obtained separately. The diamagnetic contribution of the sample itself was estimated from Pascal's constants.

X-ray Crystallography. X-ray crystallographic measurements were made on a Rigaku Raxis-Rapid imaging plate with graphite monochromated Mo Kα ($\lambda = 0.71075$ Å). Structures were determined by a direct method using SHELXS-97,[28] and refinements were performed by a full-matrix least-squares on F^2 using the SHELXL-97[29] (CrystalStructure 4.0 Crystal Structure Analysis Package, Rigaku Corporation, 2000–2010).

All non-hydrogen atoms were refined anisotropically, and all hydrogen atoms were included but not refined. Empirical absorption corrections were applied. Selected crystal data and data collection parameters are given in Tables S4 and S5 in Supplementary Information. Crystallographic data reported in this manuscript have been deposited with Cambridge Crystallographic Data Centre as supplementary publication no. CCDC-1824201–1824205. Copies of the data can be obtained free of charge via CCDC Website.

Computational Details. Density functional theory (DFT) calculations were performed using the Gaussian 03 program package.[30] The calculation was performed at the UBLYP/6-31G** level of theory with optimization of the geometries.

This work was supported by the Canon Foundation, the Grants-in-Aid for Scientific Research B (No. 25288022 and 16H04114), Elements Science and Technology Project from the Ministry of Education, Culture, Sports, Science and Technology, Japan, and Core Research for Evolutional Science and Technology (CREST) Basic Research Program "Creation of Innovative Functions of Intelligent Materials on the Basis of Element Strategy" of Japan Science and Technology Agency (JST). T.T acknowledged partially support by FIRST Quantum Information Processing Project supported by Cabinet Office, Japan, and by Grants-in-Aid for Scientific Research on Innovative Areas (Quantum Cybernetics) from the MEXT and partial support by AOARD Scientific Project on "Quantum Properties of Molecular Nanomagnets" (Award No. FA2386-13-1-4029, 4030, 4031), AOARD Project on "Molecular Spins for Quantum Technologies" (Award No. FA2386-17-1-4040).

Supporting Information

Synthetic procedures, TG/DTA profile (**1**–**6**), temporal observation and temperature dependence of UV-vis spectra (**1**–**3** and **6**), ESR spectra (**1** and **6**), magnetic susceptibility (**2**, **3** and **5**), pictures of crystal packings (**1**, **5** and **6**), UV-vis spectra in solid state (**1**–**6**), cyclic voltammograms (**1**–**6**), crystal data and selected C–C bond lengths in crystal structures (PDF). This material is available on http://dx.doi.org/10.1246/bcsj.20180074.

References

1 J. Fossey, D. Lefort, J. Sorba, *Free Radicals in Organic Chemistry*, Wiley, New York, **1997**.

2 a) *Stable Radicals: Fundamental and Applied Aspects of Odd-Electron Compounds*, ed. by R. G. Hicks, Wiley, Chichester, **2010**. doi:10.1002/9780470666975. b) *Encyclopedia of Radicals in Chemistry, Biology and Materials*, ed. by C. Chatgilialoglu, A. Studer, Wiley, Chichester, **2010**. doi:10.1002/9781119953678. c) H. G. Hicks, *Org. Biomol. Chem.* **2007**, *5*, 1321. d) R. C. Haddon, *Aust. J. Chem.* **1975**, *28*, 2343.

3 a) D. H. Reid, *Q. Rev. DC Nurses Assoc.* **1965**, *19*, 274. b) R. C. Haddon, *Nature* **1975**, *256*, 394.

4 a) Y. Morita, S. Nishida, in *Stable Radicals: Fundamental and Applied Aspects of Odd-Electron Compounds*, ed. by R. G. Hicks, Wiley, Chichester, **2010**, Ch. 3, pp. 81–145. doi:10.1002/9780470666975.ch3. b) Y. Morita, S. Suzuki, K. Sato, T. Takui, *Nat. Chem.* **2011**, *3*, 197.

5 a) V. Zaitsev, S. V. Rosokha, M. Head-Gordon, J. K. Kochi, *J. Org. Chem.* **2006**, *71*, 520. b) Z. Mou, K. Uchida, T. Kubo, M. Kertesz, *J. Am. Chem. Soc.* **2014**, *136*, 18009. c) K. Uchida, Y. Hirao, H. Kurata, T. Kubo, S. Hatano, K. Inoue, *Chem.—Asian J.* **2014**, *9*, 1823. d) K. Uchida, S. Ito, M. Nakano, M. Abe, T. Kubo, *J. Am. Chem. Soc.* **2016**, *138*, 2399. e) K. Uchida, Z. Mou, M. Kertesz, T. Kubo, *J. Am. Chem. Soc.* **2016**, *138*, 4665.

6 a) K. Goto, T. Kubo, K. Yamamoto, K. Nakasuji, K. Sato, D. Shiomi, T. Takui, M. Kubota, T. Kobayashi, K. Yakushi, J. Ouyang, *J. Am. Chem. Soc.* **1999**, *121*, 1619. b) P. A. Koutentis, Y. Chen, Y. Cao, T. P. Best, M. E. Itkis, L. Beer, R. T. Oakley, A. W. Cordes, C. P. Brock, R. C. Haddon, *J. Am. Chem. Soc.* **2001**, *123*, 3864. c) A. Ueda, S. Suzuki, K. Yoshida, K. Fukui, K. Sato, T. Takui, K. Nakasuji, Y. Morita, *Angew. Chem., Int. Ed.* **2013**, *52*, 4795.

7 Thiophenalenyl radicals without steric protection were successfully prepared and determined as discrete neutral radicals, although they readily decompose in the solution and solid states, see; a) L. Beer, S. K. Mandal, R. W. Reed, R. T. Oakley, F. S. Tham, B. Donnadieu, R. C. Haddon, *Cryst. Growth Des.* **2007**, *7*, 802. b) L. Beer, R. W. Reed, C. M. Robertson, R. T. Oakley, F. S. Tham, R. C. Haddon, *Org. Lett.* **2008**, *10*, 3121. c) P. Bag, F. S. Tham, B. Donnadieu, R. C. Haddon, *Org. Lett.* **2013**, *15*, 1198.

8 a) X. Chi, M. E. Itkis, B. O. Patrick, T. M. Barclay, R. W. Reed, R. T. Oakley, A. W. Cordes, R. C. Haddon, *J. Am. Chem. Soc.* **1999**, *121*, 10395. b) M. E. Itkis, X. Chi, A. W. Cordes, R. C. Haddon, *Science* **2002**, *296*, 1443. c) S. K. Pal, M. E. Itkis, F. S. Tham, R. W. Reed, R. T. Oakley, R. C. Haddon, *Science* **2005**, *309*, 281. d) A. Sarkar, M. E. Itkis, F. S. Tham, R. C. Haddon, *Chem.—Eur. J.* **2011**, *17*, 11576. e) P. Bag, M. E. Itkis, S. K. Pal, E. Bekyarova, B. Donnadieu, R. C. Haddon, *J. Phys. Org. Chem.* **2012**, *25*, 566. f) P. Bag, M. E. Itkis, S. K. Pal, E. Bekyarova, B. Donnadieu, R. C. Haddon, *Crystals* **2012**, *2*, 446. g) A. Sarkar, S. K. Pal, M. E. Itkis, F. S. Tham, R. C. Haddon, *J. Mater. Chem.* **2012**, *22*, 8245. h) S. K. Pal, P. Bag, M. E. Itkis, F. S. Tham, R. C. Haddon, *J. Am. Chem. Soc.* **2014**, *136*, 14738. i) M. Fumanal, J. J. Novoa, J. Ribas-Arino, *Chem.—Eur. J.* **2017**, *23*, 7772.

9 a) T. Kubo, Y. Katada, A. Shimizu, Y. Hirao, K. Sato, T. Takui, M. Uruichi, K. Yakushi, R. C. Haddon, *J. Am. Chem. Soc.* **2011**, *133*, 14240. b) T. Kubo, *Chem. Rec.* **2015**, *15*, 218.

10 a) H. M. Blatter, H. Lukaszewski, *Tetrahedron Lett.* **1968**, *9*, 2701. b) C. P. Constantinides, P. A. Koutentis, *Adv. Heterocycl. Chem.* **2016**, *119*, 173.

11 a) Y. Morita, T. Ohba, N. Haneda, S. Maki, J. Kawai, K. Hatanaka, K. Sato, D. Shiomi, T. Takui, K. Nakasuji, *J. Am. Chem. Soc.* **2000**, *122*, 4825. b) S. Nishida, J. Kawai, M. Moriguchi, T. Ohba, N. Haneda, K. Fukui, A. Fuyuhiro, D. Shiomi, K. Sato, T. Takui, K. Nakasuji, Y. Morita, *Chem.—Eur. J.* **2013**, *19*, 11904. c) Y. Morita, S. Nishida, J. Kawai, T. Takui, K. Nakasuji, *Pure Appl. Chem.* **2008**, *80*, 507.

12 a) Y. Morita, T. Aoki, K. Fukui, S. Nakazawa, K. Tamaki, S. Suzuki, A. Fuyuhiro, K. Yamamoto, K. Sato, D. Shiomi, A. Naito, T. Takui, K. Nakasuji, *Angew. Chem., Int. Ed.* **2002**, *41*, 1793. b) Y. Morita, S. Suzuki, K. Fukui, S. Nakazawa, H. Kitagawa, H. Kishida, H. Okamoto, A. Naito, A. Sekine, Y. Ohashi, M. Shiro, K. Sasaki, D. Shiomi, K. Sato, T. Takui, K. Nakasuji, *Nat. Mater.* **2008**, *7*, 48.

13 a) J. Inoue, K. Fukui, T. Kubo, S. Nakazawa, K. Sato, D. Shiomi, Y. Morita, K. Yamamoto, T. Takui, K. Nakasuji, *J. Am. Chem. Soc.* **2001**, *123*, 12702. See also, b) E. Clar, D. G. Stewart, *J. Am. Chem. Soc.* **1953**, *75*, 2667. c) N. Pavliček, A. Mistry, Z. Majzik, N. Moll, G. Meyer, D. J. Fox, L. Gross, *Nat. Nanotechnol.* **2017**, *12*, 308.

14 a) Y. Morita, S. Nishida, T. Murata, M. Moriguchi, A. Ueda, M. Satoh, K. Arifuku, K. Sato, T. Takui, *Nat. Mater.* **2011**, *10*, 947. b) S. Nishida, Y. Morita, in *Organic Redox Systems: Synthesis, Properties, and Applications*, ed. by T. Nishinaga, Wiley, Hoboken, **2016**, Ch. 6, pp. 177–243. doi:10.1002/9781118858981.ch6.

15 Y. Ikabata, Q. Wang, T. Yoshikawa, A. Ueda, T. Murata, K. Kariyazono, M. Moriguchi, H. Okamoto, Y. Morita, H. Nakai, *npj Quantum Mater.* **2017**, *2*, 27.

16 a) G. Allinson, R. J. Bushby, J.-L. Paillaud, D. Oduwole, K. Sales, *J. Am. Chem. Soc.* **1993**, *115*, 2062. b) G. Allinson, R. J. Bushby, J.-L. Paillaud, M. Thornton-Pett, *J. Chem. Soc., Perkin Trans. 1* **1995**, 385.

17 Y. Ikabata, K. Akiba, H. Nakai, *Chem. Lett.* **2013**, *42*, 1386.

18 a) A. Ueda, H. Wasa, S. Nishida, Y. Kanzaki, K. Sato, D. Shiomi, T. Takui, Y. Morita, *Chem.—Eur. J.* **2012**, *18*, 16272. b) A. Ueda, H. Wasa, S. Nishida, Y. Kanzaki, K. Sato, T. Takui, Y. Morita, *Chem.—Asian J.* **2013**, *8*, 2057.

19 a) D. Small, V. Zaitsev, Y. Jung, S. V. Rosokha, M. Head-Gordon, J. K. Kochi, *J. Am. Chem. Soc.* **2004**, *126*, 13850. b) S. Suzuki, Y. Morita, K. Fukui, K. Sato, D. Shiomi, T. Takui, K. Nakasuji, *J. Am. Chem. Soc.* **2006**, *128*, 2530. c) Z. Cui, H. Lischka, H. Z. Beneberu, M. Kertesz, *J. Am. Chem. Soc.* **2014**, *136*, 5539. d) Z. Mou, T. Kubo, M. Kertesz, *Chem.—Eur. J.* **2015**, *21*, 18230.

20 P. v. R. Schleyer, C. Maerker, A. Dransfeld, H. Jiao, N. J. R. v. E. Hommes, *J. Am. Chem. Soc.* **1996**, *118*, 6317.

21 A. Bondi, *J. Phys. Chem.* **1964**, *68*, 441.

22 a) J. B. Torrance, *Acc. Chem. Res.* **1979**, *12*, 79. b) S. Yamaguchi, Y. Moritomo, Y. Tokura, *Phys. Rev. B* **1993**, *48*, 6654. c) M. Meneghetti, *Phys. Rev. B* **1994**, *50*, 16899.

23 B. Bleaney, K. D. Bowers, *Proc. R. Soc. London, Ser. A* **1952**, *214*, 451.

24 D. C. Johnston, R. K. Kremer, M. Troyer, X. Wang, A. Klümper, S. L. Bud'ko, A. F. Panchula, P. C. Canfield, *Phys. Rev. B* **2000**, *61*, 9558.

25 J. C. Bonner, M. E. Fisher, *Phys. Rev.* **1964**, *135*, A640.

26 a) K. Kinoshita, T. Kawakami, Y. Morita, T. Saito, S. Yamanaka, M. Okumura, K. Yamaguchi, *Bull. Chem. Soc. Jpn.* **2016**, *89*, 315. See, also, b) L. Buimaga-Iarinca, C. G. Floare, C. Morari, *Chem. Phys. Lett.* **2014**, *598*, 48. c) E. F. V. de Carvalho, A. Lopez-Castillo, O. Roberto-Neto, *Chem. Phys. Lett.* **2018**, *691*, 291. d) Z. Mou, M. Kertesz, *Angew. Chem., Int. Ed.* **2017**, *56*, 10188.

27 a) D. Jérome, H. J. Schulz, *Adv. Phys.* **1982**, *31*, 299. b) *Semiconductors and Semimetals: Highly Conducting Quasi-One-Dimensional Organic Crystals*, ed. by E. M. Conwell, Academic Press, New York, **1988**, vol. 27. c) T. Ishiguro, K. Yamaji, G. Saito, *Organic Superconductors*, 2nd Ed., Springer-Verlag, Berlin, **1998**. doi:10.1007/978-3-642-58262-2.

28 G. M. Sheldrick, *Program for the Solution of Crystal Structures*, University of Göttingen, Göttingen, **1997**.

29 G. M. Sheldrick, *Program for the Refinement of Crystal Structures*, University of Göttingen, Göttingen, **1997**.

30 M. J. Frisch, G. W. Trucks, H. B. Schlegel, G. E. Scuseria, M. A. Robb, J. R. Cheeseman, J. A. Montgomery, Jr., T. Vreven, K. N. Kudin, J. C. Burant, J. M. Millam, S. S. Iyengar, J. Tomasi, V. Barone, B. Mennucci, M. Cossi, G. Scalmani, N. Rega, G. A. Petersson, H. Nakatsuji, M. Hada, M. Ehara, K. Toyota, R. Fukuda, J. Hasegawa, M. Ishida, T. Nakajima, Y. Honda, O. Kitao, H. Nakai, M. Klene, X. Li, J. E. Knox, H. P. Hratchian, J. B. Cross, V. Bakken, C. Adamo, J. Jaramillo, R. Gomperts, R. E. Stratmann, O. Yazyev, A. J. Austin, R. Cammi, C. Pomelli, J. Ochterski, P. Y. Ayala, K. Morokuma, G. A. Voth, P. Salvador, J. J. Dannenberg, V. G. Zakrzewski, S. Dapprich, A. D. Daniels, M. C. Strain, O. Farkas, D. K. Malick, A. D. Rabuck, K. Raghavachari, J. B. Foresman, J. V. Ortiz, Q. Cui, A. G. Baboul, S. Clifford, J. Cioslowski, B. B. Stefanov, G. Liu, A. Liashenko, P. Piskorz, I. Komaromi, R. L. Martin, D. J. Fox, T. Keith, M. A. Al-Laham, C. Y. Peng, A. Nanayakkara, M. Challacombe, P. M. W. Gill, B. G. Johnson, W. Chen, M. W. Wong, C. Gonzalez, J. A. Pople, *GAUSSIAN 03*, Gaussian, Inc., Wallingford, CT, **2004**.

